scientific reports

Check for updates

OPEN

# Coenzyme Q10 protects against 6 GHz electromagnetic field–induced liver injury via suppression of inflammatory responses associated with NF-κB/p65 immunoreactivity and endoplasmic reticulum stress

Kerimali Akyildiz[1]✉, Hamit Yilmaz[2], Adnan Yilmaz[3], Tolga Mercantepe[4], Fatih Gul[5] & Levent Tumkaya[6]

**We evaluated endoplasmic reticulum stress responses in hepatic tissues following 6 GHz electromagnetic field (EMF) exposure and the protective effects of Coenzyme Q10 (CoQ10). The experimental design included 24 male Sprague–Dawley rats randomly assigned to three groups: (i) sham control group, (ii) 6 GHz EMF exposure group, and (iii) 6 GHz EMF exposure + CoQ10 treatment group. Rats in the exposure groups were subjected to 6 GHz EMF exposure for 2 h/day over 30 consecutive days. Rats in the exposure groups were subjected to 6 GHz EMF exposure (0.21 mW/cm$^2$; specific absorption rate: 0.014 W/kg) for 2 h/day over 30 consecutive days. In addition, the animals in the CoQ10 treatment group received CoQ10 orally at a dose of 10 mg/kg/day throughout the exposure period. After completing the experimental protocol, hepatic tissue samples were obtained for subsequent analyses. Comparative analyses revealed significant differences in TBARS, GSH, TNF-α, IL-1β, ALT, and AST levels across the control–6 GHz and 6 GHz –6 GHz + CoQ10 groups. Exposure to 6 GHz EMF increased histopathological damage and liver histopathological score values, whereas CoQ10 markedly reduced these changes and suppressed glucose-regulated protein 78, C/EBP homologous protein, oxidative 8-hydroxy-2′-deoxyguanosine, and nuclear factor kappa B p65immunoreactivitiesy. 6 GHz EMF induces hepatic dysfunction via oxidative stress, endoplasmic reticulum stress, inflammation, and DNA damage, whereas CoQ10 mitigates these effects of EMF exposure.**

**Keywords** 6 GHz, Coenzyme Q10, Hepatotoxicity, Oxidative stress, Rat

Recent developments in wireless technology have profoundly altered communication and connectivity. This process has enabled faster and more widespread access to information, influencing various fields.[1] Recent developments have led to the rapid expansion and diversification of the application areas of wearable devices, ranging from medical monitoring systems to military communication technologies.[2] Owing to its exceptionally high data transmission speed, low latency, and continuous connectivity capabilities, 5G mobile communication

[1]Department of Medical Services and Techniques, Health Care Services Vocational School, Recep Tayyip Erdogan University, Rize, Turkey. [2]Department of Biophysics, Faculty of Medicine, Kahramanmaraş Sütçü İmam University, Kahramanmaraş, Turkey. [3]Department of Biochemistry, Faculty of Medicine, Recep Tayyip Erdogan University, Rize, Turkey. [4]Department of Histology and Embryology, Faculty of Medicine, Recep Tayyip Erdogan University, Rize, Turkey. [5]Department of Electrical and Electronics Engineering, Recep Tayyip Erdogan University, Rize, Turkey. [6]Department of Histology and Embryology, Faculty of Medicine, Ondokuz Mayıs University, Samsun, Turkey. ✉email: kerimali.akyildiz@erdogan.edu.tr

technology has become increasingly important in various aspects of daily life and has shown a growing level of integration into everyday applications. However, 5G mobile communication systems operate at higher frequency bands and involve an increased base station density. This has increased the need to investigate the biological effects of exposure to electromagnetic fields (EMF), particularly at the tissue and cellular levels[5,6].

The biological effects of EMF on tissues are associated with specific physicochemical interactions. When tissues are exposed to EMF, they interact with charged molecules and ion channels within the cell membranes, causing disruptions in the ionic balance and an increase in reactive oxygen species (ROS) production[7]. Increased ROS generation can lead to oxidative damage, including lipid peroxidation, protein damage, and compromised DNA integrity. Additionally, this process may interfere with protein folding homeostasis, potentially leading to endoplasmic reticulum (ER) stress and contributing to ER stress-associated inflammatory responses[8]. This disruption of protein-folding homeostasis is considered an important mechanism underlying the inflammatory responses and tissue damage associated with exposure to EMFs. Consequently, ER stress has been identified as a key molecular mechanism driving EMF-induced cellular stress and subsequent pathophysiological changes[9].

Experimental studies have indicated that exposure to EMF is associated with increased oxidative stress (OS), enhanced lipid peroxidation, mitochondrial dysfunction, and suppression of antioxidant defense systems in the liver of rats.[9,10] These biochemical alterations disrupt protein folding homeostasis, thereby activating ER stress responses and subsequently triggering hepatocellular injury and inflammatory processes.[10,11] Accordingly, elucidating the OS–ER stress axis associated with EMF exposure from next-generation wireless technologies, such as 5G, is critical for understanding the hepatotoxicity.[5,12,13].

Given the central role of oxidative stress and ER stress in EMF-induced tissue injury, compounds that can modulate these pathways may exert protective effects. Coenzyme Q10 (CoQ10), known for its strong antioxidant capacity, mitochondrial stabilization, and cellular stress modulation, has emerged as a promising protective agent against ER stress and oxidative damage. By supporting mitochondrial function, modulating inflammatory responses, and regulating cellular stress-related processes, CoQ10 exerts broad-spectrum protective effects in various tissues, including the cardiovascular, nervous, and hepatic systems.[14–16]

Although numerous studies have investigated the biological effects of radiofrequency electromagnetic fields (RF-EMF), knowledge regarding the 6 GHz frequency band, which is becoming increasingly important in next-generation wireless communication technologies, remains limited. Most existing studies have focused on lower frequency ranges, and the biological effects of 6 GHz RF-EMF exposure on living systems have not yet been fully elucidated. In particular, significant gaps remain in our understanding of cellular stress responses, inflammatory processes, and the interactions between these mechanisms under 6 GHz exposure. Furthermore, studies evaluating the efficacy of potential protective agents against 6 GHz RF-EMF exposure are scarce. Moreover, the potential modulatory role of CoQ10 in this context remains unclear[17,18].

This study assessed the effects of 6 GHz RF-EMF exposure on liver tissue at the biochemical, histopathological, and immunohistochemical levels. The 6 GHz frequency, part of the mid-band spectrum utilized in 5G and next-generation wireless communication systems, was chosen because of its high data transmission capacity, increasing usage potential, and limited data available on its biological effects. A daily exposure duration of 2 h was employed to create a controlled and reproducible experimental model, which is consistent with previously published RF-EMF studies. This study focused on endoplasmic reticulum (ER) stress and inflammatory processes, and examined the potential protective effects of CoQ10. This study aimed to enhance the current literature on the biological effects of 6 GHz RF-EMF exposure and the potential role of CoQ10.

## Materials and methods

### Animals

The present investigation employed cadaveric tissues remaining from a previously conducted ethics-approved study examining 6 GHz EMF-induced ER stress and the protective effects of CoQ10, which was approved by the Animal Ethics Committee of Recep Tayyip Erdogan University, Rize, Turkey (Ethics Committee Decision No. 2022/25–30.06.2022).

All Sprague Dawley rats used in this study were 3–4 months old and weighed 200–250 g at the beginning of the experiment. The animals were housed under standard laboratory conditions at the Experimental Animal Research Center of Recep Tayyip Erdogan University, Rize, Turkiye. The rats were maintained in polypropylene cages under controlled environmental conditions, including a temperature of 22 ± 2 °C, relative humidity of 50–60%, and a 12-h light/dark cycle. The animals had free access to standard laboratory chow and water ad libitum. All experimental procedures and animal care protocols were conducted in accordance with institutional guidelines and complied with the guidelines of the Animal Research: Reporting of In Vivo Experiments (ARRIVE) initiative.

### Formation of experimental groups

Rats with comparable biological and physiological characteristics, including age, body weight, male sex, and confirmed healthy status, were randomly allocated to three experimental groups (n = 8 per group) to ensure uniformity and minimize biological variability. Randomization was performed to minimize selection bias and ensure comparability between the groups.

Animals in the Sham control group received no active treatment and were administered physiological saline via oral gavage throughout the experimental period. Rats assigned to the 6 GHz group were exposed only to a 6 GHz EMF for 2 h per day between 10:00 and 12:00 AM. A 1 mL dose of corn oil, used as a vehicle for CoQ10, was administered orally via gavage to each rat at a dose of 10 mg/kg/day[15]. All treatment and exposure protocols were applied for 30 days. To minimize variability, group allocation, treatment administration, and exposure conditions were maintained under standardized and consistent conditions for the duration of the experiment.

## EMF measurement and specific absorption rate (SAR) calculation

The electromagnetic field (EMF) intensity within the exposure cage was quantified using a broadband Narda SRM-3006 EMF analyzer equipped with an isotropic antenna. Measurements were conducted at nine predetermined locations on the cage floor to evaluate the homogeneity of the field distribution. The average electric field strength obtained from these measurements was used to estimate the whole-body SAR using the equation $SAR = \sigma E^2/\rho$, where σ represents the tissue conductivity, E is the electric field strength, and ρ is the tissue density. An RF Explorer Signal Generator Combo Plus facilitated the exposure to electromagnetic waves.

The experimental groups were subjected to a 6 GHz EMF for 30 consecutive days at fixed daily intervals (10:00–12:00 AM) to ensure uniformity in all experimental conditions. The generator antenna was centrally positioned within the cage to ensure consistent exposure. The applied frequency was 6 GHz, with a power density of 0.21 $mW/cm^2$ and SAR of 0.014 W/kg, which is indicative of whole-body exposure conditions (Fig. 1).

## Tissue processing

Rats were anesthetized by intramuscular administration of ketamine (50 mg/kg) and xylazine (5 mg/kg) in accordance with standard experimental anesthesia protocols. Liver tissue specimens were systematically collected from the left lateral lobe to ensure anatomical consistency and minimize regional variability. After collection, samples designated for biochemical analyses were immediately stored at − 80 °C until further processing. After collection, samples intended for histopathological evaluation were fixed in 10% neutral-buffered formalin for 24–36hbeforeo routine tissue processing[19].

## Biochemical analysis

*Tissue homogenization*

After collection, the tissue specimens were immediately preserved at − 80 °C until analysis. On the day of the experiment, the samples were gradually thawed on ice to prevent abrupt temperature-related degradation of biomolecules. Subsequently, each specimen was weighed and homogenized in phosphate-buffered saline (PBS; pH 7.4) under cold conditions using a mechanical homogenizer at 30 Hz for 5 min. This procedure ensured adequate disruption of the tissue matrix and the release of intracellular components from the cells. The homogenates were centrifuged at 2000 × g for 10 min at 4 °C, and the clear supernatants were carefully separated from the pellets. Supernatants were used to determine the relevant biochemical parameters[20].

*Determination of thiobarbituric acid reactive substances (TBARS), glutathione (GSH), tumor necrosis factor-alpha (TNF-α), interleukin-1 beta (IL-1β), alanine aminotransferase (ALT) and aspartate aminotransferase (AST) levels*

Lipid peroxidation status was evaluated by quantifying TBARS, a secondary product of lipid oxidation, using a TBARS-based spectrophotometric method at 532 nm, and the results were reported as nmol per gram of tissue[21].

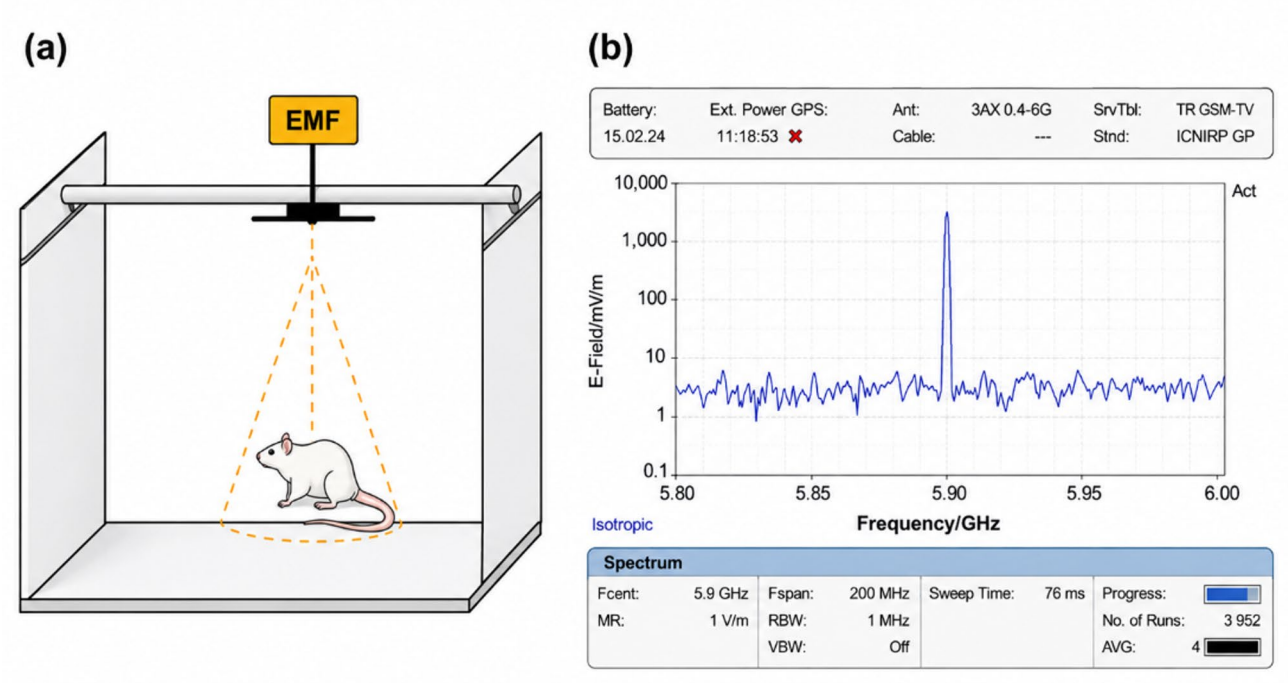



**Fig. 1**. (**a**) Design of the Experimental EMF Exposure Cage, (**b**) Narda SRM-3006 measurement of the EMF spectrum.

The GSH levels in the liver tissue were determined using the Ellman method. Tissue samples were homogenized in PBS (pH 7.4), and proteins were precipitated by adding trichloroacetic acid and centrifuging. The resulting supernatant was reacted with DTNB, and the absorbance was measured at 412 nm wavelength. The results were calculated using a standard curve and expressed as nmol/g tissue[22].

The pro-inflammatory cytokines TNF-α and IL-1β were assessed in the tissue samples using rat-specific ELISA kits (E-EL-R2856 and E-EL-R0012). Absorbance values obtained at 450 nm were used to generate standard curves, from which analyte concentrations were calculated and presented in pg/g of tissue. TNF-α and IL-1β levels were determined using commercially available ELISA kits (Elabscience Biotechnology Co., Ltd.). (Wuhan, China) according to the manufacturer's protocols. ALT and AST levels were measured using an automated biochemical analyzer (Architect c8000; Abbott Laboratories, Abbott Park, IL, USA).

## Histopathological analyses

*Histopathological staining*

Liver tissues were harvested from anesthetized animals and promptly trimmed to approximately 1.5 $cm^3$ while being kept moist with physiological saline solution. The samples were subsequently fixed in 10% neutral-buffered formalin (Sigma-Aldrich, St. Louis, MO, USA), prepared with phosphate buffer for 24–36 h. Post-fixation, routine histological processing was performed using a tissue processor (Citadel 2000; Thermo Scientific, Waltham, MA, UK).

The liver tissue samples were dehydrated using a graded ethanol series comprising 50%, 70%, 80%, 90%, 96%, and two changes of 100% ethyl alcohol (Merck KGaA, Darmstadt, Germany). Following dehydration, the tissues were cleared using two changes of xylene (Merck KGaA, Darmstadt, Germany). Subsequently, the liver tissue samples were infiltrated with soft and hard paraffin (Merck KGaA, Darmstadt, Germany). After paraffin infiltration, the tissue samples were embedded in hard paraffin using embedding cassettes and a tissue-embedding station (Leica EG1150 H; Leica Biosystems, Germany). Paraffin blocks derived from liver tissues were sectioned to a thickness of 4–4.5 µm using a rotary microtome (Leica RM2125RT, Germany).

The sections were stained with Hematoxylin–Eosin (H&E) using Harris hematoxylin (Merck, Germany) and Eosin G (Merck KGaA, Darmstadt, Germany), as well as with Masson's trichrome stain (Merck KGaA, Darmstadt, Germany). Stained liver tissue sections were examined under a light microscope (Olympus BX51, Olympus Corporation, Tokyo, Japan), and photomicrographs were captured using an Olympus DP74 digital camera (Olympus Corporation, Tokyo, Japan).

*Immuno-histochemical analysis*

Immunohistochemistry was performed to evaluate ER stress, oxidative DNA damage, and inflammation in liver tissue. ER stress markers were detected using primary antibodies against glucose-regulated protein 78 (GRP78; sc-13539, Santa Cruz Biotechnology, USA) and C/EBP homologous protein (CHOP; E-AB-70087, Elabscience, USA). Oxidative DNA damage was assessed using an anti 8-hydroxy-2′-deoxyguanosine (8-OHdG; sc-66036, Santa Cruz Biotechnology, USA) antibody. Inflammatory responses were evaluated using a nuclear factor kappa B p65 antibody (NF-κB p65 [E379], ab325367; Abcam, UK).

Paraffin-embedded liver Sects. (2–3 µm) were immune-stained using an automated system (Bond Max, Leica Biosystems), visualized with DAB, counterstained with Harris hematoxylin, and examined by light microscopy.

*Semi-quantitative analysis*

Rat liver histopathological damage was evaluated using a semi-quantitative scoring system based on vacuolated cytoplasm with anisonuclear hepatocytes, sinusoidal dilatation, and inflammation scores. The resulting liver histopathological score (LHS) (Table 1) was independently assessed by two blinded histopathologists who examined 50 randomly selected microscopic fields per rat.

Liver tissue sections from each rat incubated with GRP-78, CHOP, 8-OHdG, and NF-κB/p65 primary antibodies were analyzed for the number of positively stained cells by two blinded histopathologists (Table 2). For each specimen, 50 randomly selected fields were evaluated to determine the immunohistochemical (IHC) positivity score[24–27].

## Statistical assessment

Prior to statistical analysis, data normality was assessed using the Shapiro–Wilk test. Biochemical data that showed a normal distribution were analyzed using one-way analysis of variance (ANOVA), followed by Tukey's HSD post hoc test to determine the differences between groups.

Histopathological data that were non-normally distributed or ordinal in nature were analyzed using the Kruskal–Wallis test. When significant differences were detected, Dunn's multiple comparison test was performed for post-hoc analysis (Table 3).

Data are presented as mean ± standard deviation (SD) or median (minimum–maximum), as appropriate. Statistical significance was set at $p < 0.05$. All statistical analyses were performed using IBM SPSS Statistics (version XX; IBM Corp., Armonk, NY, USA).

# Results

## Biochemical findings

Tissue ALT, AST, TBARS, GSH, TNF-α, and IL-1β levels differed significantly in comparisons involving the 6 GHz group ($p < 0.05$), and no significant differences were observed between the control and 6 GHz + CoQ10 groups in the analyzed parameters ($p > 0.05$).

| Severity | Percentage % | Score |
|---|---|---|
| *Hepatocellular vacuolization with anisokaryosis* | | |
| Absent | < 5 | 0 |
| Mild | 5–25 | 1 |
| Moderate | 26–50 | 2 |
| Severe | 51–75 | 3 |
| Very severe | > 75 | 4 |
| *Sinusoidal dilatation* | | |
| Absent | < 5 | 0 |
| Mild | 5–25 | 1 |
| Moderate | 26–50 | 2 |
| Severe | 51–75 | 3 |
| Very severe | > 75 | 4 |
| *Inflammatory cell infiltration* | | |
| Absent | < 5 | 0 |
| Mild | 5–25 | 1 |
| Moderate | 26–50 | 2 |
| Severe | 51–75 | 3 |
| Very severe | > 75 | 4 |

**Table 1**. Semi-quantitative scoring criteria used for the calculation of the LHS.[23]. *The Total LHS was calculated as the sum of the scores for hepatocellular vacuolization with anisokaryosis, sinusoidal dilatation, and inflammatory cell infiltration. Accordingly, the total LHS ranged from 0 to 12, with higher scores indicating greater histopathological liver injury.

| Severity | Percentage % | Score |
|---|---|---|
| *Immun-Positivity Hepatocytes* | | |
| Absent | < 5 | 0 |
| Mild | 5–25 | 1 |
| Markedly | 26–50 | 2 |
| Severe | 51–75 | 3 |
| Very severe | > 75 | 4 |

**Table 2**. Immune-Positivity Scoring Methods.

| Group | TBARS (nmol/g tissue) | GSH (nmol/g tissue) | TNF-α (pg/g tissue) | IL-1β (pg/g tissue) | ALT (U/L) | AST (U/L) |
|---|---|---|---|---|---|---|
| Sham Control | 16.27 ± 1.67 | 25.16 ± 2.59 | 57.30 ± 4.01 | 82.66 ± 4.41 | 40.5 ± 4.4 | 47.12 ± 6.17 |
| 6 GHz | 22.13 ± 2.32* | 20.75 ± 3.50* | 63.30 ± 3.74* | 90.72 ± 4.32* | 56 ± 3.97* | 60.5 ± 4.78* |
| 6 GHz + CoQ10 | 17.61 ± 3.08# | 25.30 ± 2.01# | 58.09 ± 3.04# | 84.87 ± 2.82# | 43.75 ± 4.71# | 46.77 ± 3.79# |

**Table 3**. Biochemical Parameters in the Study Groups (mean ± SD). *$p < 0.05$, compared with the sham control group. #$p < 0.05$, compared with the 6 GHz group.

## Histopathological findings

Histological assessment by light microscopy demonstrated preserved Remak's cords and normal sinusoidal architecture in the sham control group (Fig. 2A, Table 4). In contrast, the 6 GHz-exposed group exhibited marked histopathological alterations, including anisokaryotic hepatocytes, cytoplasmic vacuolization, sinusoidal dilatation, and inflammatory cell infiltration, resulting in significantly liver injury compared with the sham control group (Fig. 2B, Table 4). CoQ10 treatment substantially attenuated these histopathological changes and improved the overall hepatic architecture compared to the 6 GHz group (Fig. 2C, Table 4). The detailed histopathological scores are presented in Table 4.

## Immunohistochemical (IHC) findings

GRP-78 immunoreactivity was evaluated in liver sections to assess endoplasmic reticulum stress after 6 GHz EMF exposure. The control samples showed immunonegative hepatocytes with preserved morphology (Fig. 3A and Table 5). In contrast, the 6 GHz group exhibited increased GRP-78 immunopositivity in hepatocytes within

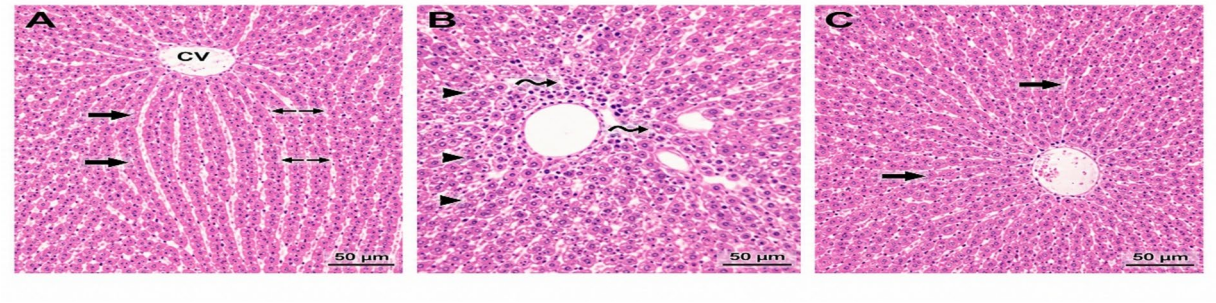



**Fig. 2**. Representative histopathological findings in rat liver tissue (H&E staining, × 200). (**A**) Sham control group showing preserved hepatic architecture, intact Remak's cords (thick arrows), and normal sinusoidal spaces (thin arrows) surrounding the central vein (CV). (**B**) The 6 GHz EMF group showed sinusoidal dilatation (wavy arrows) and inflammatory cell infiltration (arrowheads). (**C**) 6 GHz EMF + CoQ10 group demonstrating partial restoration of hepatic architecture and reduced histopathological alterations (arrows).

| Group | Hepatocellular vacuolization with anisokaryosis | Sinusoidal Dilataion | Inflammation | LHS |
|---|---|---|---|---|
| Sham Control | 0(0–0) | 0(0–0) | 0(0–0) | 0(0–1) |
| 6 GHz | 2(2–2)[a] | 2(2–2)[a] | 1(1–2)[a] | 5(5–6)[a] |
| 6 GHz + CoQ10 | 1(0–1)[b] | 0(0–1)[b] | 0(0–1)[b] | 1(0–2)[b,c] |

**Table 4**. Histopathology Scores (HS; median and interquartile range [25–75%]). [a]$P = 0.001$ compared with the Sham control group, [b]$P = 0.001$ compared with the 6 GHz group, [c]$P = 0.018$ compared with the Sham control group,

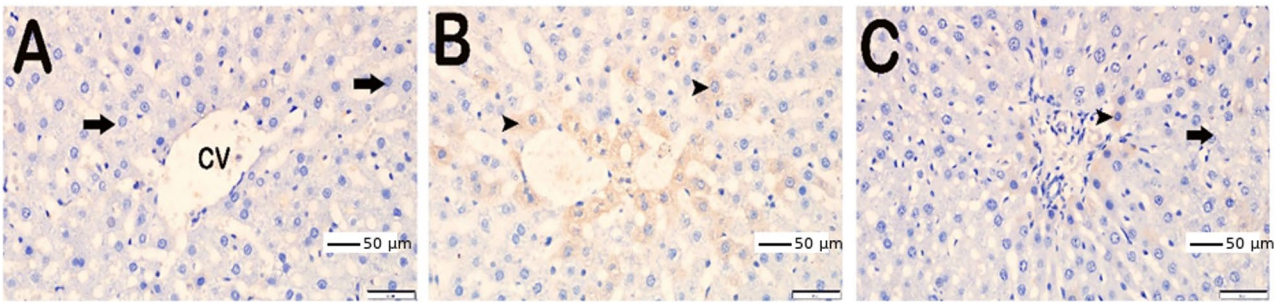



**Fig. 3**. Representative GRP-78–immune-stained liver sections from 6 GHz EMF–exposed rats were observed under light microscopy. (**A**) (× 40), Sham control group: Intact hepatocytes within Remak's cords showing negative GRP-78 staining (arrows). (**B**) (× 40), 6 GHz group: Increased GRP-78 immunopositivity in hepatocytes located within the intralobular regions of Remak's cords (arrowheads). (**C**) (× 40), 6 GHz + CoQ10 group: Markedly reduced GRP-78 immunoreactivity compared with the 6 GHz group, indicating the attenuation of ER stress following CoQ10 treatment (arrows).

| Group | Grp-78 Positivity Score | CHOP Positivity Score | 8-OHdG Positivity Score | NF-Kβ/p65 Positivity Score |
|---|---|---|---|---|
| Sham Control | 0(0–0) | 0(0–0) | 0(0–1) | 0(0–0) |
| 6 GHz | 1(1–2)[a] | 2(2–2)[a] | 2(2–3)[a] | 0.5(0–1)[a] |
| 6 GHz + CoQ10 | 0(0–0)[b] | 0(0–1)[b,c] | 1(1–1)[b,d] | 0(0–0)[e] |

**Table 5**. Semi-Quantitative Analysis Results (Median-25%-75% interquartile range). [a]$P = 0.001$ compared with the Sham control group, [b]$P = 0.001$ compared with the 6 GHz group, [c]$P = 0.02$ compared with the Sham control group, [d]$P = 0.02$ compared with the 6 GHz group, [e]$P = 0.16$ compared with the 6 GHz group,

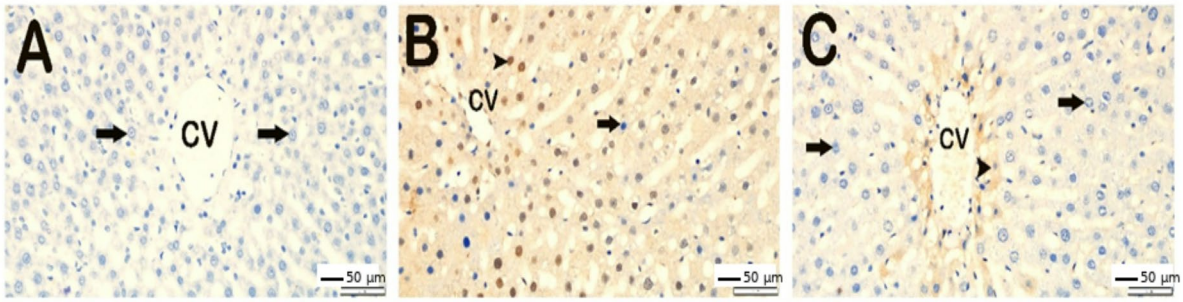



**Fig. 4**. Representative CHOP-immunostained liver sections from rats exposed to 6 GHz EMF under light microscopy. (**A**) (×40), Sham control group: Intact hepatocytes within Remak's cords indicate negative CHOP staining (arrow), corresponding to a positivity score of 0 (0–0). (**B**) (×40) Central Vein (CV), 6 GHz group: İmmunopositive hepatocytes situated in the intralobular regions of Remak's cords indicate low-level CHOP immunopositivity (arrowhead), corresponding to a positivity score of 1 (1–2). (**C**) (×40), 6 GHz + CoQ10 group: İmmunopositive hepatocytes in the Remak's cords indicated negligible CHOP immunoreactivity, corresponding to a positivity score of 0 (0–1).

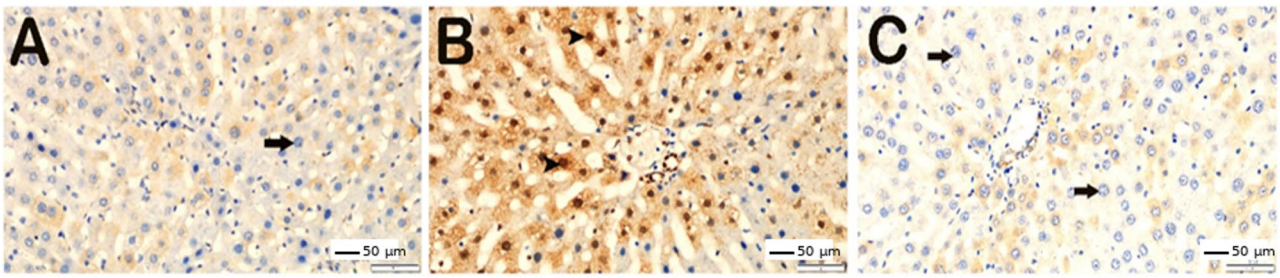



**Fig. 5**. Representative 8-OHdG–immune-stained liver sections from 6 GHz EMF–exposed rats under light microscopy. (**A**) (×40), Sham control group: Intact hepatocytes within the Remak's cords indicate negative 8-OHdG staining (arrow), corresponding to a positivity score of 0 (0–1). (**B**) (×40), 6 GHz group: Poptotic hepatocytes situated in the intralobular regions of Remak's cords indicate moderate-level 8-OHdG immunopositivity (arrowhead), corresponding to a positivity score of 2 (2–3). (**C**) (×40), 6 GHz + CoQ10 group: İmmunopositive hepatocytes in Remak's cords exhibited intermediate-level 8-OHdG immunoreactivity, corresponding to a positivity score of 1 (1–1).

the intralobular regions, indicating enhanced ER stress (Fig. 3B; Table 5). CoQ10 treatment markedly reduced GRP-78 immunoreactivity compared to the 6 GHz group (Fig. 3C, Table 5). The detailed immunopositivity scores are presented in Table 5.

CHOP immunoreactivity was assessed in liver sections to evaluate endoplasmic reticulum stress after 6 GHz EMF exposure. No CHOP-immunopositive hepatocytes were observed in the sham control group (Fig. 4A and Table 5). In contrast, the 6 GHz-exposed group exhibited marked CHOP immunopositivity in hepatocytes, indicating enhanced ER stress (Fig. 4B; Table 5). CoQ10 administration attenuated CHOP expression, particularly within the intralobular Remak's cords, compared to the 6 GHz group (Fig. 4C, Table 5). The detailed immunopositivity scores are presented in Table 5.

8-OHdG immunoreactivity was evaluated in liver sections to assess oxidative DNA damage after 6 GHz EMF exposure. Control samples predominantly showed immunonegative hepatocytes within the intralobular Remak's cords (Fig. 5A, Table 5). In contrast, the 6 GHz group exhibited a marked increase in 8-OHdG immunopositive hepatocytes, particularly within the intralobular regions, indicating enhanced oxidative damage (Fig. 5B, Table 5). CoQ10 treatment attenuated 8-OHdG immunoreactivity compared with the 6 GHz group (Fig. 5C, Table 5). Detailed immunopositivity scores are presented in Table 5.

NF-κB/p65 immunoreactivity was assessed in liver sections to evaluate the inflammatory responses following 6 GHz EMF exposure. The control samples showed immunonegative hepatocytes within Remak's cords (Fig. 6A, Table 5). In contrast, the 6 GHz-exposed group exhibited increased NF-κB/p65 immunopositivity in hepatocytes, predominantly within the intralobular regions, indicating enhanced inflammation (Fig. 6B, Table 5). CoQ10 administration attenuated NF-κB/p65 immunoreactivity compared to the 6 GHz group (Fig. 6C and Table 5). Detailed immunopositivity scores are presented in Table 5.

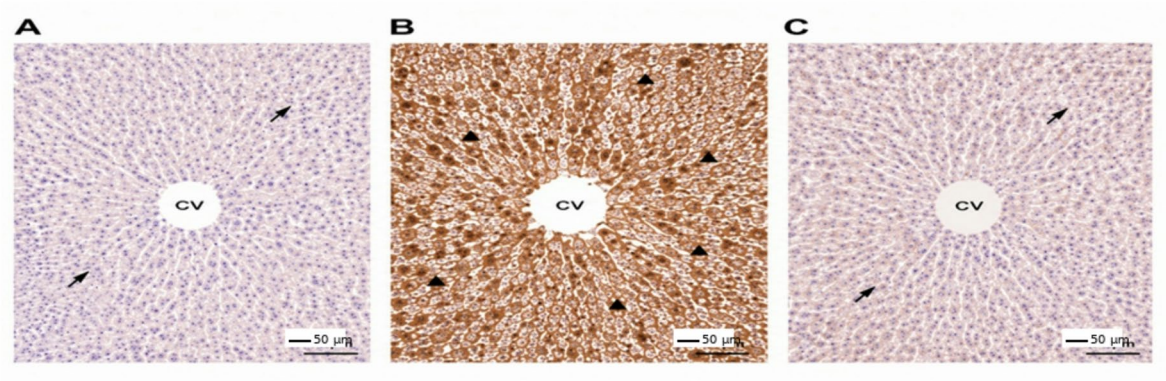



**Fig. 6**. Representative NF-κB/p65–immune-stained liver sections from 6 GHz EMF–exposed rats under light microscopy. (**A**) (×40), Sham control group: Intact hepatocytes within Remak's cords indicate NF-κB/p65 immunonegativity (arrow), with a positivity score of 0 (0–0). (**B**) (×40) Central Vein (CV), 6 GHz group: Immunopositive hepatocytes situated in the intralobular regions of Remak's cords indicate moderate-level NF-κB/p65 immunopositivity (arrowhead), corresponding to a positivity score of 0.5 (0–1). (**C**) (×40), 6 GHz + CoQ10 group: İmmunopositive hepatocytes in the Remak's cords indicated intermediate-level NF-κB/p65 immunoreactivity, corresponding to a positivity score of 0 (0–0).

## Discussion

The environmental electromagnetic landscape has changed significantly owing to ongoing technological advancements, which have increased the number of EMF sources. Notably, the rapid growth in mobile phone usage, one of the most swiftly advancing technologies, has resulted in a steady rise in daily EMF exposure, sparking concerns about possible negative health effects[28,29].

Exposure to 6 GHz-related radiofrequency EMFs may compromise hepatocellular integrity by activating OS, inflammatory cascades, and ER stress pathways. Accordingly, this study investigated the molecular mechanisms underlying this effect in liver tissue and assessed whether CoQ10, a mitochondrial antioxidant, could attenuate EMF-induced hepatic injury.

OS is a key pathophysiological process that triggers ER stress and apoptosis through increased lipid peroxidation and suppression of antioxidant defense mechanisms. Numerous studies on different tissues and organs have indicated that OS-related increases in lipid peroxidation, together with reductions in antioxidant capacity, are closely associated with ER stress responses and cellular death pathways[30,31].

The findings of the present study indicate that 6 GHz electromagnetic field exposure triggers multiple interconnected pathological processes in the hepatic tissue. The increase in TBARS levels, along with a decrease in GSH levels following exposure, demonstrates the development of a pronounced oxidative stress response in the liver. Concurrent increases in GRP78 and CHOP immunoreactivity suggest that oxidative stress may contribute to the activation of endoplasmic reticulum stress pathway. Similarly, elevated levels of TNF-α, IL-1β, and NF-κB/p65 indicate the involvement of inflammatory responses in this process. The simultaneous increase in oxidative stress, endoplasmic reticulum stress, and inflammatory markers, along with enhanced 8-OHdG immunoreactivity, further suggests the presence of oxidative DNA damage at the cellular level. The association between these biochemical and immunohistochemical alterations and increased liver histopathological injury scores indicates that the observed molecular changes are accompanied by structural tissue damage. In contrast, CoQ10 administration reduced TBARS levels while preserving GSH concentrations, suppressed inflammatory mediators and endoplasmic reticulum stress markers, and markedly alleviated histopathological damage. Taken together, these findings suggest that 6 GHz EMF exposure promotes a pathophysiological axis involving oxidative stress, endoplasmic reticulum stress, and inflammation in hepatic tissue, whereas CoQ10 exerts protective effects at multiple stages of this interconnected pathway.

Previous research has established that exposure to electromagnetic radiation (EMR) at frequencies of 900, 1800, and 2100 MHz results in a significant elevation of TBARS levels in rat liver tissue, accompanied by reductions in GSH, ALT, and AST levels, indicating a compromised antioxidant defense capacity[32]. Notably, the extent of TBARS elevation and thiol depletion has been reported to increases with higher exposure frequencies[33]. Similarly, exposure to 1800 MHz has been shown to elevate hepatic TBARS levels while significantly reducing GSH concentrations[34]. Consistent with these findings, the pronounced increase in TBARS levels observed in this study suggests that EMR exposure induces oxidative stress. This interpretation is supported by the concurrent reduction in GSH levels, which is one of the major components of the cellular antioxidant defense system. Together, these findings indicate a disturbance in the oxidant–antioxidant balance and suggest the presence of oxidative damage in liver tissue following EMR exposure.

Moreover, the lack of specific measurements of reduced and oxidized glutathione (GSH/GSSG) levels, as well as the activities of key enzymes involved in glutathione redox metabolism, such as glutathione peroxidase and glutathione reductase, constitutes a significant limitation of the present study. The inclusion of these parameters would facilitate a more comprehensive assessment of antioxidant defense mechanisms. Additionally, previous

studies have suggested that exposure to EMF induces inflammatory responses through cellular stress-related processes, resulting in alterations in proinflammatory cytokine profiles[35–37].

Consistent with these findings, the increase in proinflammatory cytokine levels observed in our study suggests that EMF exposure disrupts oxidative balance and may contribute to inflammation-related cellular stress. Increased production of reactive oxygen species (ROS) following EMF exposure may disturb protein folding homeostasis and contribute to endoplasmic reticulum (ER) stress. The unfolded protein response (UPR), activated under ER stress, is mainly regulated through three canonical pathways: protein kinase RNA-like endoplasmic reticulum kinase (PERK), inositol-requiring enzyme 1 (IRE1), and activating transcription factor 6 (ATF6). Although this adaptive response initially aims to restore cellular homeostasis, persistent stress may promote the involvement of redox-sensitive transcription factors such as NF-κB, potentially enhancing the expression of inflammatory mediators. This mechanism suggests a reciprocal interaction between oxidative stress and inflammation. Accordingly, the elevated proinflammatory cytokine levels observed in our study support the potential involvement of ROS generation, ER stress–related responses, and UPR-associated inflammatory processes in liver tissue following EMF exposure, which is consistent with previous experimental findings.

Mechanistically, ER stress may contribute to inflammation through several interconnected signaling pathways. Activated IRE1α interacts with TRAF2, leading to the activation of JNK and NF-κB signaling, whereas PERK activation may promote inflammatory responses through eIF2α phosphorylation and ATF4-mediated transcriptional regulation[38,39]. In addition, prolonged CHOP activation may exacerbate cellular dysfunction and inflammatory signaling. In the present study, the concomitant increase in GRP78, CHOP, TNF-α, IL-1β, and NF-κB/p65 immunoreactivity following 6 GHz EMF exposure is consistent with the potential involvement of ER stress–associated inflammatory pathways in hepatic injury[11,40].

Our findings are consistent with those of numerous studies reporting histological alterations in the liver tissue following EMF exposure. In one study, higher median levels of portal inflammation, single-cell necrosis, vascularity, and congestion were reported in the 6 GHz RF-EMR group than in the controls[41]. Similarly, another study indicated moderate sinusoidal hyperemia and dilation in the livers of rats following exposure to 2.45-GHz EMR[42]. In another study investigating 900/1800-MHz and 2.4-GHz frequencies, RF-EMR exposure induced marked lobular inflammatory changes in liver tissue[43].

Experimental evidence indicates that EMF exposure within the 900–2100 MHz frequency range may induce frequency-dependent structural alterations in liver tissue, accompanied by increased oxidative stress and activation of inflammatory pathways in the liver. These histopathological changes include disruption of the hepatic cord architecture, central vein obstruction, increased cytoplasmic eosinophilia, sinusoidal dilatation, and enhanced Kupffer cell activation, all of which reflect progressive hepatic injury associated with EMF-induced oxidative imbalance[33]. Similarly, previous studies have indicated that 1800 MHz EMR exposure can result in pronounced sinusoidal dilatation, central vascular compression, and significant impairment of hepatocyte integrity, primarily mediated by inflammation and oxidative damage[44]. Collectively, these findings support the notion that EMF-related oxidative and inflammatory processes may contribute to the structural and functional disturbances in hepatic tissue.

The liver histopathological findings reported in the literature are consistent with the increases in portal inflammation, single-cell necrosis, vascularity, and congestion observed after 6 GHz RF-EMR exposure in this study. These findings suggest that, despite differences in the frequencies applied, EMFs exposure may induce hepatic injury through shared pathophysiological mechanisms, primarily mediated by enhanced oxidative stress and activation of inflammatory responses, and underscore the importance of considering the potential impact of high-frequency RF-EMR exposure on liver health.

In one study, rats were exposed to EMR for at least one week (2 h/day), and apoptosis was assessed using caspase-12 and cleaved caspase-3, whereas ER stress–related oxidative responses were evaluated via GRP78 and CHOP proteins. Exposure to 900 and 2100 MHz RFR for 1 or 10 weeks resulted in significant upregulation of GRP78 and CHOP expression[30], along with marked increases in cleaved caspase-3 and caspase-12 levels.

This may promote the expression of proinflammatory genes and enhance reactive oxygen species production. Therefore, it can be suggested that EMF-induced inflammatory responses may involve the ER stress–NF-κB–microglia axis, and targeting this multifaceted mechanism may hold promise for developing potential protective strategies. Accumulating evidence indicates that DNA damage can potentiate cellular injury by promoting inflammation-related responses, including the cGAS–STING axis[45,46].

In experimental models, Wistar rats exposed to 915 MHz radiofrequency radiation showed a significant increase in liver DNA damage[47]. The accumulation of experimental data indicates that exposure to EMF leads to various forms of DNA damage, including single- and double-strand breaks and DNA–protein crosslinks, which collectively intensify DNA damage–related cellular stress[48–50].

The findings of the present study are largely consistent with those of previous studies on EMF-induced molecular and cellular response. In particular, the upregulation of ER stress responses mediated by GRP78 and CHOP, activation of inflammation via NF-κB/p65, and oxidative DNA damage reflected by increased 8-OHdG levels collectively indicate that 6 GHz RF-EMF exposure triggers a multifaceted cellular stress response in the liver tissue. These results support the notion that EMFs may exert their effects through shared pathophysiological mechanisms, irrespective of frequency, and highlight the central role of the ER stress–inflammation–oxidative damage axis in this process.

Moreover, the improvements observed following CoQ10 administration suggest that its hepatoprotective effects may be mediated by the attenuation of oxidative stress, endoplasmic reticulum stress, and inflammation. As a potent antioxidant and an essential component of the mitochondrial electron transport chain, CoQ10 may help preserve the cellular redox balance and limit the activation of stress-related signaling pathways[51,52]. Previous studies have reported that CoQ10 can modulate the unfolded protein response signaling, including the PERK, IRE1, and ATF6 pathways, thereby reducing inflammatory responses. Consistent with these mechanisms,

CoQ10 treatment in the present study was associated with reduced GRP78, CHOP, NF-κB/p65, TNF-α, IL-1β, and 8-OHdG levels, suggesting an overall protective effect against EMF-induced hepatic injury[52,53].

## Strengths and limitations

This study had several limitations. This study was conducted using a single animal model with a relatively small sample size, and EMF exposure was limited to a specific frequency, duration, and power density. In addition, CoQ10 was evaluated at a single dose, precluding the assessment of dose–response relationships, and a CoQ10-only group was not included in the experimental design of this study. Consequently, the independent effects of CoQ10 on liver tissue and the extent to which the observed improvements in the EMF + CoQ10 group were attributable to the intrinsic effects of CoQ10 rather than its interaction with EMF exposure could not be determined. Furthermore, correlation analyses of oxidative stress markers, endoplasmic reticulum stress indicators, inflammatory mediators, and histopathological injury scores were not performed. Such analyses may provide additional mechanistic insights into the relationships among these parameters and further clarify the biological pathways underlying EMF-induced hepatic injury. Moreover, the expression of NF-κB/p65, GRP78, and CHOP was evaluated solely by immunohistochemistry, and no additional validation was performed using quantitative molecular techniques, such as western blotting or RT-qPCR. Therefore, future studies incorporating these methods will provide further confirmation of the molecular mechanisms underlying the observed findings. Nevertheless, the combined use of biochemical, histopathological, and immunohistochemical analyses enabled a comprehensive evaluation at the tissue level. However, further experimental and clinical studies are warranted to validate these findings and comprehensively elucidate the underlying mechanisms.

## Conclusions

These results indicate that EMF exposure exacerbates hepatocellular alterations not only through oxidative stress but also via ER stress and associated inflammatory responses. The reduction in lipid peroxidation, partial restoration of antioxidant balance, and suppression of pro-inflammatory cytokines in the CoQ10-treated group indicated its protective effects, which were further supported by the histopathological findings.

## Data availability

The datasets generated during and/or analysed during the current study are available from the corresponding author on reasonable request.

Received: 17 April 2026; Accepted: 19 June 2026
Published online: 22 June 2026

## References

1. Korkmaz, E. et al. 6 GHz NR RF-EMF exposure assessment technologies review. *Environ. Res.* **260**, 119524 (2024).
2. Gallucci, S. et al. Assessment of EMF human exposure due to wearable antennas at 5 G frequency band. *Sensors* **23**(1), 104 (2022).
3. Agrawal, V., Agrawal, S., Bomanwar, A., Dubey, T. & Jaiswal, A. Exploring the risks, benefits, advances, and challenges in internet integration in medicine with the advent of 5G technology: A comprehensive review. *Cureus* **15**(11), e48767 (2023).
4. Zreikat, A. I. et al. IoT integration in 5G networks. *Computers* **14**(7), 250 (2025).
5. Puginier, E. et al. Biological effects of 5G-modulated 700 MHz RF-EMF exposure on neuronal and glial cell models under isothermal conditions. *Sci. Rep.* **16**(1), 10767 (2026).
6. Salem, M. A. et al. EMF-aware radio resource management for 5G. *Computers* **14**(2), 51 (2025).
7. Panagopoulos, D. J., Karabarbounis, A., Yakymenko, I. & Chrousos, G. P. Human-made electromagnetic fields: Ion forced-oscillation and voltage-gated ion channel dysfunction, oxidative stress and DNA damage (Review). *Int. J. Oncol.* **59**(5), 92 (2021).
8. Matsushima, G. et al. Endoplasmic reticulum stress and unfolded protein response in immune cell function. *Front. Immunol.* **16**, 1694102 (2025).
9. Cao, Y. et al. STING contributes to lipopolysaccharide-induced tubular cell inflammation and pyroptosis by activating endoplasmic reticulum stress in acute kidney injury. *Cell Death Dis.* **15**(3), 217 (2024).
10. Teranishi, M. et al. Extremely low-frequency electromagnetic field (ELF-EMF) increases mitochondrial electron transport chain activities and ameliorates depressive behaviors in mice. *Int. J. Mol. Sci.* **25**(20), 11315 (2024).
11. Baydar, A. T. et al. L arginine and radiofrequency electromagnetic field attenuate inflammatory and apoptotic injury after experimental subarachnoid hemorrhage. *Sci. Rep.* https://doi.org/10.1038/s41598-026-56001-x.Advanceonlinepublication (2026).
12. Zhang, M. et al. De novo transcriptome profiling reveals the bioeffect of the clam (Cyclina sinensis) to graded extremely low-frequency electromagnetic fields (ELF-EMF, 50 Hz) exposure. Environmental pollution (Barking, Essex : 1987), 128472. Advance online publication (2026).
13. Tumkaya, L. et al. Prenatal EMF effects on rat livers. *Cells Tissues Organs* **207**(3–4), 187–196 (2019).
14. Zhang, S. et al. CoQ10 alleviates hepatic ischemia reperfusion injury via inhibiting NLRP3 activity and promoting Tregs infiltration. *Mol. Immunol.* **155**, 7–16 (2023).
15. Bagheri, S. et al. Neuroprotective effects of coenzyme Q10 on neurological diseases: A review article. *Front. Neurosci.* **17**, 1188839 (2023).
16. Littarru, G. P. & Tiano, L. Antioxidant properties of CoQ10. *Mol Biotechnol* **37**(1), 31–37 (2007).
17. Karamazı, Y. et al. Effect of 6 GHz radiofrequency electromagnetic field on the development of fetal bones. *Electromagn Biol Med.* **44**(1), 17–25 (2025).
18. Emre, M. et al. Effect of high-frequency radiofrequency (6 GHz) electromagnetic radiation on oxidative stress and kidney morphology. *Toxicol Ind Health.* **42**(4), 124–136 (2026).
19. Yilmaz, A. et al. The hepatoprotective effects of camellia sinensis on cisplatin-induced acute liver injury. *Life* **14**(9), 1077 (2024).
20. Deniz, E., Topcu, A., Ozturk, A., Ozturk, S. D. & Akyildiz, K. Hedera helix folium extract attenuates methotrexate-induced hepatotoxicity by modulating oxidative stress and inflammatory mediators. *Tissue Cell* **96**, 102967 (2025).
21. Draper, H. H. & Hadley, M. Malondialdehyde determination as index of lipid peroxidation. *Methods Enzymol.* **186**, 421–431 (1990).
22. Ellman, G. L. Tissue sulfhydryl groups. *Arch. Biochem. Biophys.* **82**(1), 70–77 (1959).
23. Ciftel, S. et al. Protective effects of trimetazidine and dexmedetomidine on liver injury in a mesenteric artery ischemia-reperfusion rat model via endoplasmic reticulum stress. *Biomedicines* **12**(10), 2299 (2024).

24. Gokce, Y., Seker, U. & Pekince Ozoner, M. Safety analysis of ELF-PEMF in rat liver. *Hepatol Forum* **5**(4), 178–183 (2024).
25. Haroon, A., Ali, S., Umar, U., Farooq, S., Fahad, T., & Qureshi, T. Histopathological effects of 4G and 5G electromagnetic radiations on liver tissue. J Rawalpindi Med College (2025).
26. Meyer, F. et al. RF-EMF effects on OS biomarkers: systematic review. Environ Int, 194 (2024).
27. Yava, M. RF radiation effects on rat liver and PON1. Ann Med Res, 30(10) (2023).
28. Yilmaz, A. et al. Prenatal mobile phone exposure hepatotoxicity. *J Matern-Fetal Neonatal Med* **30**(11), 1355–1359 (2017).
29. Wang, A. S., Savla, P., Brazdzionis, J., Ko, K. & Miulli, D. E. Optimal voltage for cranial electromagnetic field stimulation to modulate brain activity. *Cureus* **17**(4), e82011 (2025).
30. Kaya, E. et al. RF radiation-induced ER stress in rat thymus. *Eur Res J* **9**(1), 29–38 (2023).
31. Paul, B. et al. Paraoxonase-like APMAP maintains endoplasmic-reticulum-associated lipid and lipoprotein homeostasis. *Dev. Cell* **60**(17), 2313-2330.e10 (2025).
32. Gunes, M. et al. An Evaluation of the genotoxic effects of electromagnetic radiation at 900 MHz, 1800 MHz, and 2100 MHz frequencies with a SMART assay in *Drosophila melanogaster*. *Electromagn. Biol. Med.* **40**(2), 254–263 (2021).
33. Sharma, A., Shrivastava, S. & Shukla, S. RF-EMF oxidative damage in rat liver and brain. *Free Radic Res.* **55**(5), 535–546 (2021).
34. Berköz, M. et al. 1800 MHz radio-frequency electromagnetic radiation induces OS in rat liver, kidney and brain tissues. *East J Med* **23**(2), 71–78 (2018).
35. Bouji, M., Lecomte, A., Hode, Y., de Seze, R. & Villégier, A. S. Effects of 900 MHz radiofrequency on corticosterone, emotional memory and neuroinflammation in middle-aged rats. *Exp. Gerontol.* **47**(6), 444–451 (2012).
36. Megha, K. et al. Microwave radiation-induced OS in rat brain. *Neurotoxicology* **51**, 158–165 (2015).
37. Singh, K. V. et al. Mobile phone radiation effects in rats. *Environ. Sci. Pollut. Res.* **27**(16), 19340–19351 (2020).
38. Elshazly, N. F. et al. Ambroxol alleviates hippocampus injury after BRIR through suppression of the IRE1α/TRAF2 signaling pathway. *Life Sci.* **379**, 123875 (2025).
39. Mo, H. et al. Inhibition of PA28γ expression can alleviate osteoarthritis by inhibiting endoplasmic reticulum stress and promoting STAT3 phosphorylation. *Bone Joint Res* **13**(11), 659–672 (2024).
40. Kandemir, Ö. et al. Nephroprotective effects of hesperidin on ifosfamide-induced acute nephrotoxicity in rats: Role of NF-κB/ TNF-α/ IL-1β, p53/caspase-3/Bax/Bcl-2, and ATF6/IRE1/PERK/GRP78 signaling pathways. *Arch. Biochem. Biophys.* **770**, 110465 (2025).
41. Ilgaz, N. S. et al. Genotoxic and histopathological effects of 6 GHz RF-EMR on rat liver. *Electromagn. Biol. Med.* **44**(4), 472–483 (2025).
42. Kesari, K. K., Behari, J. & Kumar, S. Mutagenic response of 245 GHz radiation exposure on rat brain. *Int J Radiat Biol* **86**(4), 334–343 (2010).
43. Borzoueisileh, S. et al. Assessment of function, histopathological changes, and OS in liver tissue due to ionizing and non-ionizing radiations. *Caspian J. Intern. Med.* **11**(3), 315–323 (2020).
44. Adebayo, E. A., Adeeyo, A. O., Ogundiran, M. A. & Olabisi, O. Bio-physical effects of radiofrequency electromagnetic radiation (RF-EMR) on blood parameters, spermatozoa, liver, kidney and heart of albino rats. *J King Saud Univ-Sci* **31**(4), 813–821 (2019).
45. Zhang, Y. et al. Tryptanthrin targets GSTP1 to induce senescence and increases the susceptibility to apoptosis by senolytics in liver cancer cells. *Redox Biol.* **76**, 103323 (2024).
46. Sun, S. et al. Gasdermin-E-mediated pyroptosis drives immune checkpoint inhibitor-associated myocarditis via cGAS-STING activation. *Nat. Commun.* **15**(1), 6640 (2024).
47. Trosić, I., Pavicić, I., Milković-Kraus, S., Mladinić, M. & Zeljezić, D. Effect of electromagnetic radiofrequency radiation on the rats' brain, liver and kidney cells measured by comet assay. *Coll. Antropol.* **35**(4), 1259–1264 (2011).
48. Jin, H. et al. Protective effects of EMF-LTE against DNA damage. *Int. J. Mol. Sci.* **22**(10), 5134 (2021).
49. Panagopoulos, D. J. et al. Human-made EMFs, OS and DNA damage. *Int. J. Oncol.* **59**(5), 92 (2021).
50. Worel, N. et al. EMF impact on DNA damage. *Toxicol. In Vitro* **100**, 105902 (2024).
51. Abdel-Rasol, M. A. et al. Coenzyme Q10 protects against atorvastatin-induced hepatotoxicity via attenuation of oxidative stress and functional modulation of CYP3A1. *BMC Pharmacol. Toxicol.* **27**(1), 63 (2026).
52. Wang, Y., Lilienfeldt, N. & Hekimi, S. Understanding coenzyme Q. *Physiol. Rev.* **104**(4), 1533–1610 (2024).
53. Zhang, Y. et al. Discovering the potential value of coenzyme Q10 in oxidative stress: Enlightenment from a synthesis of clinical evidence based on various population. *Front. Pharmacol.* **13**, 936233 (2022).


## Acknowledgements

This study has been supported by the Recep Tayyip Erdoğan University Development Foundation (Grant Number: 020260060190403).

## Author contributions

Conceptualization, H.Y. and F.G.; methodology, H.Y., F.G., and L.T.; software, K.A.; validation, L.T., T.M., and H.Y.; formal analysis, K.A.; investigation, H.Y., F.G., and A.Y.; resources, H.Y., T.M., and L.T.; data curation, K.A.; writing—original draft preparation, K.A.; writing—review and editing, K.A.; H.Y, and L.T.; project administration, H.Y.; funding acquisition, K.A. All authors have read and agreed to the published version of the manuscript.

## Funding

This research was funded by the Scientific Research Projects Coordination Unit (BAP) of Recep Tayyip Erdoğan University (TSA-2023-1477).

## Declarations

## Competing interests

No conflicts of interest are reported by the authors.

## Ethical approval

The present investigation utilized cadaver liver tissues obtained from a previously conducted, ethics-approved study examining 6 GHz RF-EMF–induced ER stress and the potential protective effects of CoQ10 (Ethics Committee Decision No. 2022/25). These tissues were used in accordance with ethical guidelines, and all biochemical, histopathological, and immunohistochemical analyses performed in this study were conducted independently, in line with the specific objectives of this investigation. In accordance with the 3R principles

(Replacement, Reduction, and Refinement), the present study utilized cadaveric tissues remaining from a previously approved experimental study investigating 6 GHz EMF-induced endoplasmic reticulum stress and the protective effects of CoQ10. The original study was approved by the Animal Experiments Ethics Committee of Recep Tayyip Erdoğan University, Rize, Türkiye (Approval No. 2022/25, dated 30 June 2022).

## Additional information

**Correspondence** and requests for materials should be addressed to K.A.

**Reprints and permissions information** is available at www.nature.com/reprints.

**Publisher's note** Springer Nature remains neutral with regard to jurisdictional claims in published maps and institutional affiliations.

**Open Access** This article is licensed under a Creative Commons Attribution-NonCommercial-NoDerivatives 4.0 International License, which permits any non-commercial use, sharing, distribution and reproduction in any medium or format, as long as you give appropriate credit to the original author(s) and the source, provide a link to the Creative Commons licence, and indicate if you modified the licensed material. You do not have permission under this licence to share adapted material derived from this article or parts of it. The images or other third party material in this article are included in the article's Creative Commons licence, unless indicated otherwise in a credit line to the material. If material is not included in the article's Creative Commons licence and your intended use is not permitted by statutory regulation or exceeds the permitted use, you will need to obtain permission directly from the copyright holder. To view a copy of this licence, visit http://creativecommons.org/licenses/by-nc-nd/4.0/.

© The Author(s) 2026